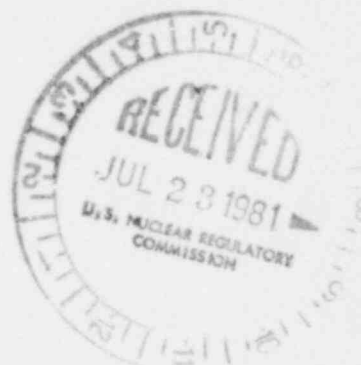


---

---

# Droplet Distributions in Open Pipes and Simulated Rod Bundles



---

---

Prepared by R. V. Smith, R. D. Lindsted

Department of Mechanical Engineering  
Wichita State University

Prepared for  
U.S. Nuclear Regulatory  
Commission

NOTICE

This report was prepared as an account of work sponsored by an agency of the United States Government. Neither the United States Government nor any agency thereof, or any of their employees, makes any warranty, expressed or implied, or assumes any legal liability or responsibility for any third party's use, or the results of such use, of any information, apparatus product or process disclosed in this report, or represents that its use by such third party would not infringe privately owned rights.

Available from

GPO Sales Program  
Division of Technical Information and Document Control  
U. S. Nuclear Regulatory Commission  
Washington, D. C. 20555

Printed copy price: \$2.75

and

National Technical Information Service  
Springfield, Virginia 22161

# Droplet Distributions in Open Pipes and Simulated Rod Bundles

---

Manuscript Completed: November 1980  
Date Published: July 1981

Prepared by  
R. V. Smith, R. D. Lindsted

Student Contributors  
M. Paddock, G. Lindsted, D. Evans, J. Salisbury, F. Shen

Department of Mechanical Engineering  
Wichita State University  
Wichita, KS 67208

Prepared for  
Division of Accident Evaluation  
Office of Nuclear Regulatory Research  
U.S. Nuclear Regulatory Commission  
Washington, D.C. 20555  
NRC FIN B6250

## ABSTRACT

Results of droplet size distributions are reported for varying conditions of air-water flow and conduit geometry. Geometry variations were open pipe and the pipe containing simulated nuclear rod bundles with various support structures.

The experimental tests showed the gas velocity to be the primary variable influencing droplet size. The Hinze (1949) expression generally predicted the effective droplet size as a function of lower gas velocities. The Hinze (1949) correlation, however, showed the droplet size as a function of  $u_g^2$ . The exponent (2) appeared to be too high.

At higher gas velocities, the Hinze (1949) correlation failed and this appeared to indicate a change in the breakup mechanism for the higher gas velocities.

The droplet size change with respect to changes in geometry and mixture quality was small. It fell in the general range of the uncertainty for the data.

## TABLE OF CONTENTS

	PAGE
LIST OF FIGURES. . . . .	vii
INTRODUCTION . . . . .	1
GENERAL REMARKS REGARDING DATA . . . . .	2
Reliability. . . . .	2
Droplet Shape. . . . .	2
Effect of Quality. . . . .	3
Droplet Size Distribution. . . . .	3
DROPLET SIZE AS A FUNCTION OF GAS VELOCITY . . . . .	4
Proposed Mechanisms and Correlations . . . . .	4
Comparisons of the "Bag Breakup" Correlation . . . . .	5
Comparison of Predictions from the Turbulent Fluctuation Correlation. . . . .	6
Comparisons with all Similar Reported Data . . . . .	6
DROPLET SIZE WITH RESPECT TO GEOMETRY CHANGES. . . . .	7
Open Tube and Simulated Rods . . . . .	7
Droplet Concentration Change in Flow through the Rod Bundle.	7
SUMMARY. . . . .	8
NOMENCLATURE . . . . .	10
REFERENCES . . . . .	11

## LIST OF FIGURES

Figure	Page
Single camera flow loop. . . . .	12
Double camera axial-viewing apparatus. . . . .	13
Simulated nuclear fuel rod bundle with metal grid strap network for the double camera loop. . . . .	14
Tracing of axial photograph of open tube . . . . .	15
Tracing of axial photograph of open tube . . . . .	16
Tracing of axial photograph of open tube . . . . .	17
Tracing of axial photograph of open tube . . . . .	18
Tracing of axial photograph of open tube . . . . .	19
Division of droplet breakup mechanism from Azzopardi et al (1980). 20	20
Comparison of experimental data with results from equation (1) . . 21	21
Comparison of experimental and calculated values of $d_{32}$ . . . . . 22	22
Comparison of all reported experimental data from similar systems. 23	23
Droplet diameter ( $d_{10}$ ) ratios to show geometry effect. . . . . 24	24
Droplet diameter distribution in flow cross section. . . . . 25	25
Droplet diameter distribution in flow cross section. . . . . 26	26
Droplet diameter distribution in flow cross section. . . . . 27	27
Flow area distributions for figures 10, 11, 12, and 14 . . . . . 28	28
Hydraulic diameters for inner and outer areas of tube bundle . . . 29	29

## DROPLET DISTRIBUTIONS IN OPEN PIPES AND SIMULATED ROD BUNDLES

### INTRODUCTION

This report summarizes a study to determine droplet sizes and geometric positions with respect to variables in gas velocity and geometry, including open pipes and simulated rod bundles. The fluids were air and water and the droplet data were obtained by means of axial photography. Complete details of the project may be found in the final NRC report dated July 1980.

Single and double camera flow loops were applied as shown in Figs. 1 and 2. In the single camera loop, the photographs were at approximately focal length from the camera, at the exit of the rod bundle. This loop had the advantage of an entrance length of at least 50 diameters. The double camera flow loop shown in Fig. 2 provided photographs both at the rod bundle entrance and at the exit. However, it had a very short entrance length which was necessitated by the geometry requirements and the focal length of the cameras. Fig. 3 shows the rod bundle with the grid installed in the tube of approximately 2-inch inside diameter. In addition to this geometry, tests were run on rod bundles without the grid (the rods were held in place by small pins to provide minimum flow disturbance), and data were obtained additionally for 2-inch open tubes and for 1-1/4-inch open tube runs.

For each run condition of fixed gas velocity, fluid quality, and geometrical arrangement, droplets were recorded by size and radial position. These droplet data were placed on computer cards to provide capability for analysis of the size and geometrical distributions with respect to the experimental variables of gas velocity and geometry. The total range of gas velocity

was approximately 7 to 22 m/s. The simulated rod bundles were, however, in a gas velocity range of 13 to 17 m/s. The total range of qualities was from about 20% to 90%, but for the simulated rod bundles was at 40%, 55%, and 70% quality. Figures 4a, b, c, d, and e show typical tracings of droplet photographs as they were prepared for data reduction. The droplet size was assumed to be roughly elliptical and the major and minor axes were recorded. It was assumed that the droplet shape would be approximately that of an ellipsoid and from that an effective droplet diameter was determined and that diameter is reported in the subsequent sections.

#### GENERAL REMARKS REGARDING DATA

##### Reliability

When the droplet data are reduced to an effective diameter such as the Sauter mean diameter ( $d_{32}$ ), the reliability is assessed on the basis of the number of droplets analyzed. Using the system outlined by Bowen and Davies (1951), the general accuracy of our reported values of  $d_{32}$  is  $\pm 6\%$ . The enormous effort associated with the photography and the manual reduction of the data limited the number of droplet sizes analyzed for each run, and thus limited the reliability for the data of this report.

##### Droplet Shape

Figure 4 shows that the droplets were not spherical. Our judgement was that they should be recorded as a general ellipsoid with data for the major and minor axes. For all experimental flow cases, the ratio of the minor axis to the major axis was approximately 0.6. There has been some concern regarding the apparent conflict between our data and others who generally report spherical droplets. It is possible that droplet radial



motion could cause a spherical droplet to appear elliptical on a photograph taken in a finite time period. Granting this however, it was thought that surely this radial velocity effect on droplet shape would be different for open tube data and for the rod bundle geometries. The invariant axis ratio was interpreted to show that the ellipticity reported was to a major extent a reasonable representation of the droplet shape. As stated previously, the data were subsequently reduced to an effective spherical diameter.

#### Effect of Quality

In all of the test conditions reported, both of geometry and of gas velocity variations, it was not possible to determine any pronounced change in the droplet data as a function of the fluid quality. Indications of quality variations were in all cases within the range of the scatter of the droplet data. Therefore, the data reported are for all qualities grouped together as a single run condition.

#### Droplet Size Distribution

Size distribution of the droplet samples was analyzed only to the point of showing a general indication that the reported distributions are similar to those which have been previously reported. Preliminary examination of the data indicated that it followed the general distribution as proposed by Rosin and Rammler (1933).

## DROPLET SIZE AS A FUNCTION OF GAS VELOCITY

Proposed Mechanisms and Correlations

This report considered two general regions of droplet breakup mechanisms which in turn determine the droplet size. In dealing with these mechanisms and proposed correlations one assumes that the data are in an equilibrium or steady state condition, which may or may not have been the actual condition for our runs. It is not believed that any difference from the steady state or equilibrium condition will significantly affect the results of the data reported here. The two droplet breakup mechanisms considered were the "bag breakup" as proposed by Hinze (1949), and the turbulent fluctuation breakup as reported by Azzopardi et al (1980). The factors which determine the general region where "bag breakup" is predominant and turbulent fluctuation is predominant are assumed to be a function of the liquid quality (or liquid flux velocity) and the gas (or gas flux velocity). A general curve separating these regions has been proposed by Azzopardi et al (1980) and is shown with our data range in Figure 5. The curve indicating the divisions was primarily chosen by examination of the character of the waves at the liquid film. Higher gas velocities in general produced "cleaner" wave patterns, and this suggested that in the region of "cleaner" wave patterns the turbulent fluctuation breakup would be predominant. Conversely, in the lower gas velocity region the wave form would be "messy" and the "bag breakup" mechanism would be predominant.

In the "bag breakup" region, Hinze (1949) assumed that droplet breakup would be governed by the balance between the forces of the pressure difference across the drop and the surface tension forces. This produced the equation

$$We_{crit} = \frac{\rho_G \Delta u_G^2 d_{max}}{\sigma_L} = 13. \quad (1)$$

The Sauter mean diameters ( $d_{32}$ ) were determined in the left part of the figure by first determining  $d_{\max}$  (approximated by  $d_{99.99\%}$ ) from the Rosin and Rammler (1933) distribution. This was further reduced by the distribution-determined relationship that  $d_{32}$  is equal to  $d_{\max}/5.14$ .

The turbulent fluctuation breakup mechanism and expression is based on the idea that breakup will occur when the imposed frequency due to turbulence becomes equal to the natural frequency of the drop. This produced the expression

$$\frac{d_{32}}{d_t} = a \frac{Re^{0.1}}{We^{0.6}} \frac{\rho_G^{0.6}}{\rho_L} + \frac{bG_{LE}}{\rho_L u_G} \quad (2)$$

This expression is from Azzopardi et al (1980).

Figure 5 shows that our data are far to the left of the proposed division line and suggests that bag breakup is the primary means of determination of droplet size for all of our data. This also appears to be borne out by the tracings shown in Figure 4 which appear to suggest that the primary breakup is from very large droplets formed by initial shearing from large or "messy" waves.

#### Comparisons of the "Bag Breakup" Correlation

Figure 6 shows the comparisons of all of the data of this report (with all qualities lumped together) with the general predictions from equation (1). At the lower gas velocities (8 to 12 m/s), equation (1) predicts the correct general range for droplet diameters. Equation (1) however, underpredicts the droplet size at the higher gas velocities. This suggests that the velocity squared term, while tending to predict the correct general range for the effective droplet diameter, begins to fail for gas velocities greater than droplet diameter, 12 m/s. This in turn suggests that the droplet breakup mechanism begins to change in the 12 m/s range. There will be further

comments regarding this in the discussion of Figure 8.

#### Comparison of Predictions from the Turbulent Fluctuation Correlation

Figure 7 shows the comparison of the experimental data with the predictions from equation (2). Clearly the substantial deviation of the data from the required agreement shown by the 45° line indicates that this correlation, and subsequently this mechanism are not appropriate for the data reported here. The droplet sizes are much larger than those predicted by equation (2).

#### Comparisons with all Similar Reported Data

Figure 8 shows the extremes of diameters and velocities for all reported data for similar systems (vertical flow with air-water as the fluids). First it may be seen that our data represents a lower velocity range than any of the other report data. The general trend connecting the data of this report to the other reported data is reasonably well-described by equation (1). For the higher gas velocity data shown, the droplet diameters appear to be predicted better as a function of  $1/(\text{gas velocity})^1$ , rather than  $(\text{gas velocity})^2$  in equation (1). The exponent of 1 was generally suggested in reviewing all reported droplet data by Smith and Azzopardi (1978). This may suggest that the transition from the "bag breakup" assumptions of Hinze (1949) may begin at lower gas velocities than those shown in Figure 5. The data presented do not lend themselves to a clear conclusion regarding these previous observations. It does seem clear, however, that reasonably reliable predictions may be obtained from equation (1) for the general region of lower gas velocities used in this project (8-12 m/s). Beyond that region, equation (1) tends to underpredict droplet size.

## DROPLET SIZE WITH RESPECT TO GEOMETRY CHANGES

### Open Tube and Simulated Rods

Figure 9 shows the droplet size ratios for the open tube, the phantom tube, and the simulated fuel rods with the grid (Fig. 4). The round symbols show data from the double camera loop recording the inlet and outlet droplet size through the rod bundles. The remaining symbols show the data from the single camera loop indicating ratios of droplet sizes for the various geometries. At the outset it should be noted that the total range shown in Figure 9 is not very great. This indicates that a reduction in droplet size is noticeable as the geometry becomes more complex, but that the ratio is in the range of 0.9 regardless of the geometry changes observed. Thus the predominant conclusion is that the droplet size change is relatively small with respect to quite a wide range of changes of geometry.

### Droplet Concentration Change in Flow through the Rod Bundle

A significant change in the droplet population with respect to radial position is shown in Figures 10, 11, and 12. These data were taken from the double camera loop that shows the rearrangement in the geometrical droplet distribution between the entrance and exit of the simulated rod bundle with grid. This change in droplet population with respect to position appeared to be rather dramatic. Comparisons between the outlet data from the single camera loop and the double camera loop showed similarities indicating that this distribution change occurred roughly the same in both loops. This change could have a significant effect on other experiments using simulated rod bundles placed in relatively small tubes.

It was thought that the change in population might be simply because the flow near the center part of the simulated bundle met with less surface resistance than that toward the outer side of the containing tube. Therefore the tube bundle was divided into two areas, shown as Area I and Area II in Figure 13, and the hydraulic diameter computed for each section. The results for the two sections are shown in Figure 14. They indicate that the hydraulic diameter relationship in the rod bundle approximately matches the droplet distribution and probably explains the change in distribution in going through the grid.

#### SUMMARY

The data of this report led to the following observations:

1. In the region of lower (8 to 12 m/s) gas flow velocities and geometries tested, the Hinze (1949) equation (1) correlation serves reasonably well to predict the effective droplet size ( $d_{32}$ ).
2. In looking at all data for droplet size, that is with the inclusion of higher gas velocities recorded, it would appear that equation (1) does not describe data at higher gas velocities (above 12 m/s). This supports the concept of a mechanism change between low velocity and high velocity droplet breakup. At the higher gas velocities the effective droplet diameter varies at the gas velocity to a power less than 2 as shown in equation (1).
3. The droplet size change with respect to changes in geometry does not appear to be very great. This seems surprising considering the major geometry changes which were tested. However, all of the data show a relatively small change, ( $d_{\text{complex geometry}}/d_{\text{simple geometry}} \approx 0.9$ ).

4. Flow through a simulated rod bundle changes the droplet population distribution with respect to radial position. The droplets are more numerous toward the center of the bundle at the outlet of the simulated rod bundle. This change of distribution appears to be a result of the larger hydraulic diameter for the flow area near the center of the bundle.

## NOMENCLATURE

a	constant
b	constant
$d_{32}$	Sauter mean diameter
$d_{MAX}$	maximum drop diameter
$d_t$	tube diameter
$G_{LE}$	entrained liquid mass flux (flow rate/unit area)
$G_G$	Gas mass flux
$G_L$	Liquid mass flux
$u_G$	gas velocity
$\rho_G$	density of gas phase
$\rho_L$	density of liquid phase
$\sigma$	surface tension
Re	gas phase Reynolds number ( $= \rho_G u_G d_t / \mu_G$ )
We	Weber number ( $= \rho_G u_G^2 d_t / \sigma$ )



## REFERENCES

Azzopardi, B.J., Freeman, G., and Whalley, P.B., (1978), "Drop sizes in annular two-phase flow," UKAEA Report AERE-R 9074.

Azzopardi, B.J., Freeman, A., and King, D.J., (1980), "Drop sizes and deposition in annular two-phase flow," (UK) AERE Report #9634.

Bowen, I.G., and Davis, G.P., (1951), "Particle Size Distribution and the Estimation of Sauter Mean Diameter," Shell Technical Report, No. ICT/28.

Cousins, L.B., and Hewitt, G.F., (1968), "Liquid phase mass transfer in annual two-phase flow: droplet deposition and liquid entrainment," UKAEA Report AERE-R 5657.

Hinze, J.O., (1949), "Forced deformation of viscous liquid globules," Applied Science Review, Vol. A1.

Namie, S., and Ueda, T., (1972), "Droplet transfer in two-phase annular mist flow," Bull. J.S.M.E., Vol. 15, p. 1568.

Smith, R.V., and Azzopardi, B.J., (1978), "Summary of reported droplet size distribution data in dispersed two-phase flow." NUREG/CR-0630. Also (UK) AERE Report No. 3020, (1979). \*

Whalley, P.B., Azzopardi, B.J., Pshyk, L., and Hewitt, G.F., (1977), "Axial view photography of waves in annular two-phase flow," UKAEA Report AERE-R 8787.

\*Available for purchase from the National Technical Information Service, Springfield, VA 22161.

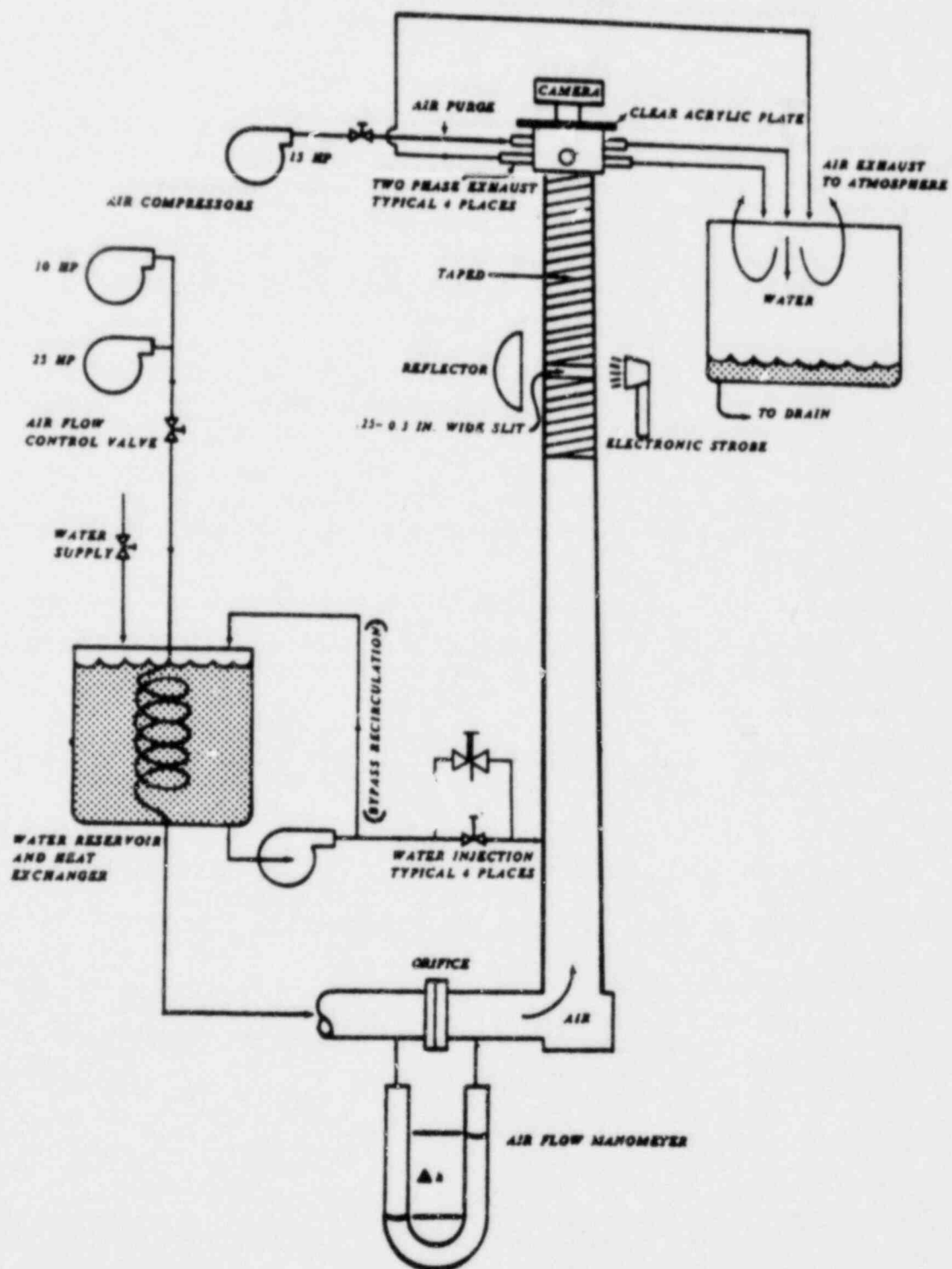


Figure 1. Single camera flow loop.

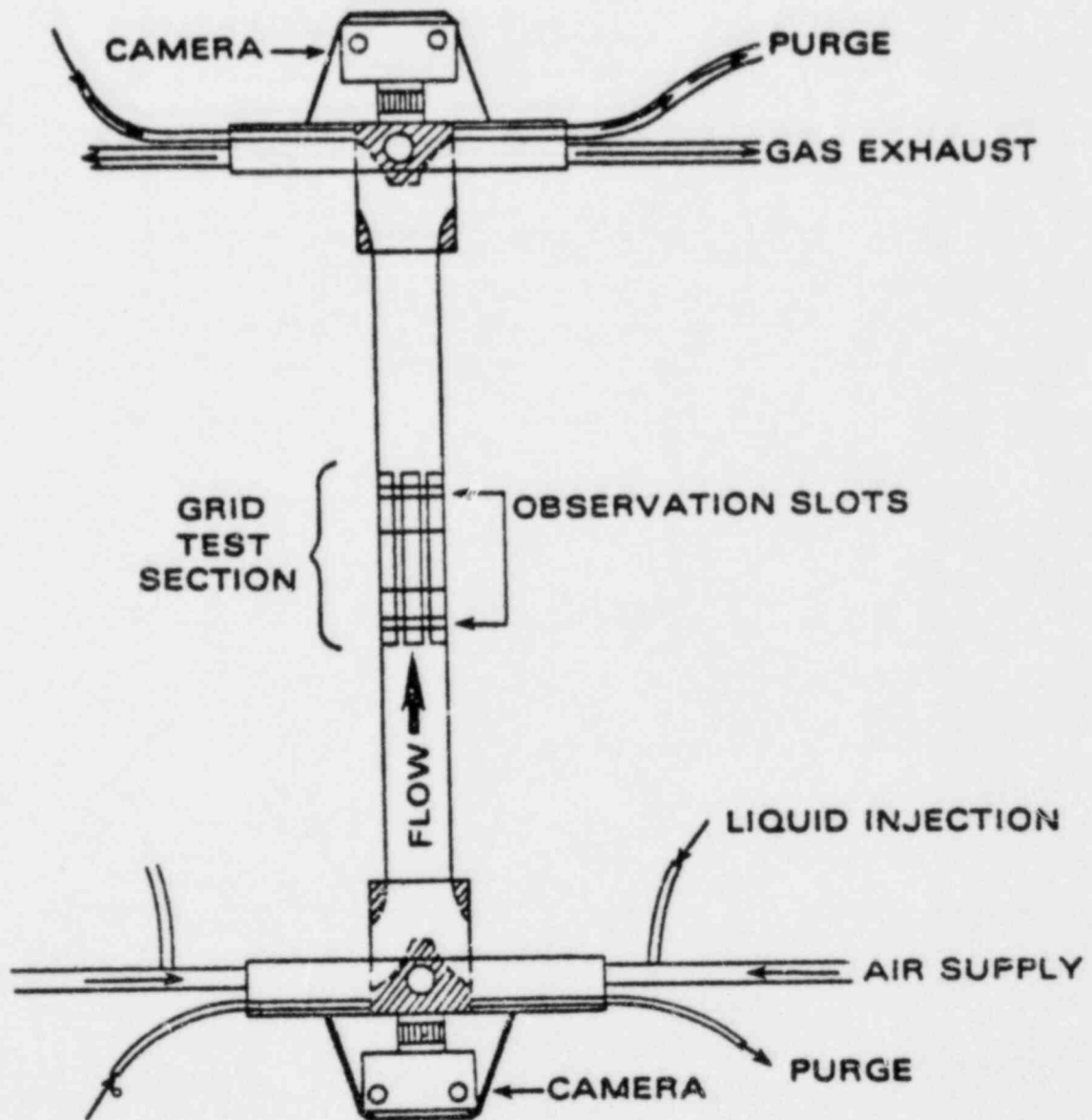


Figure 2. Double camera axial-viewing apparatus for obtaining both entrance and exit photographs of a single test grid section.

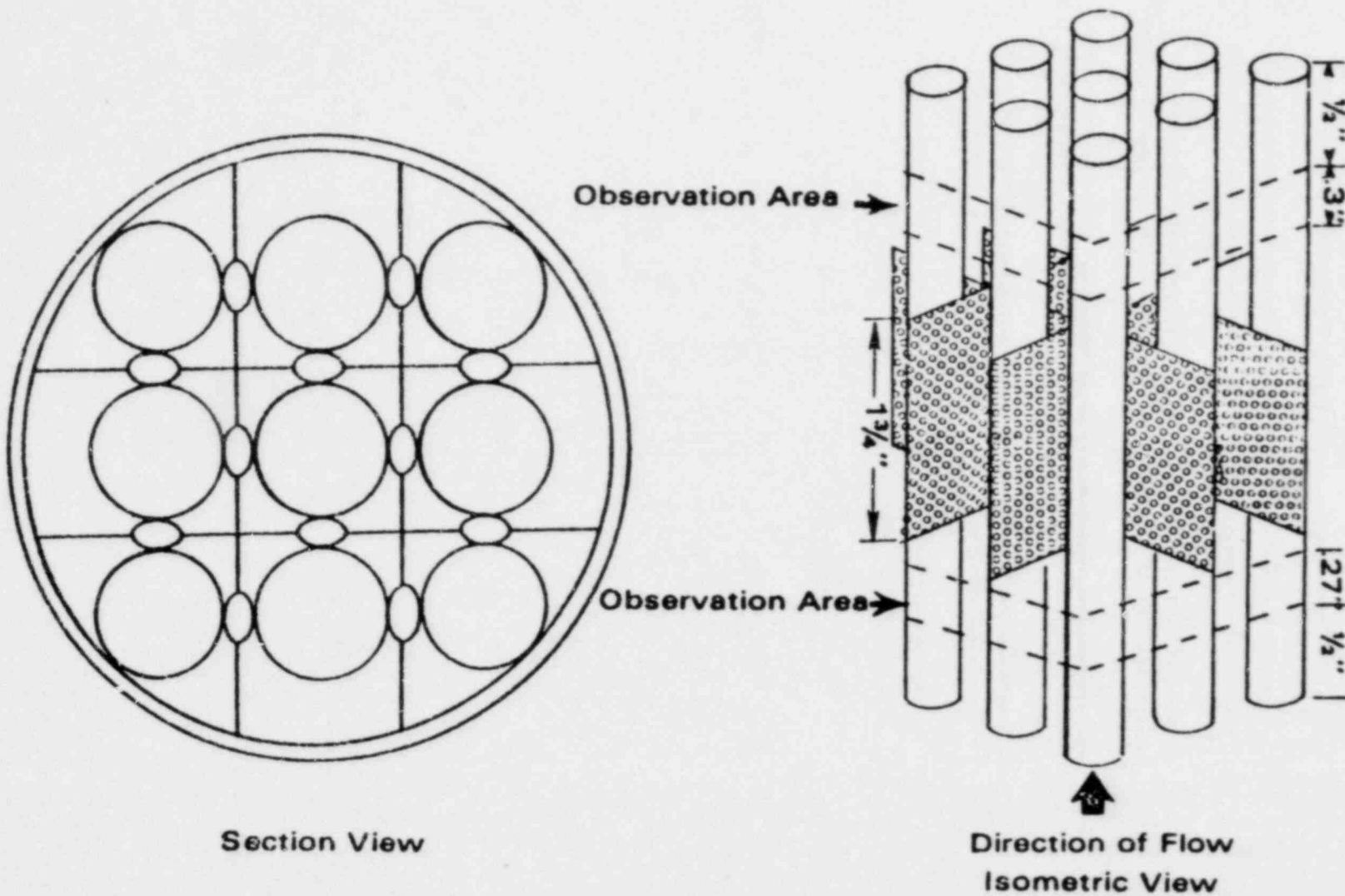


Figure 3. Simulated nuclear fuel rod bundle with metal grid strap network for the double camera loop. This assembly is labeled "Grid" rod bundle held in place by pins is labeled "Phantom."

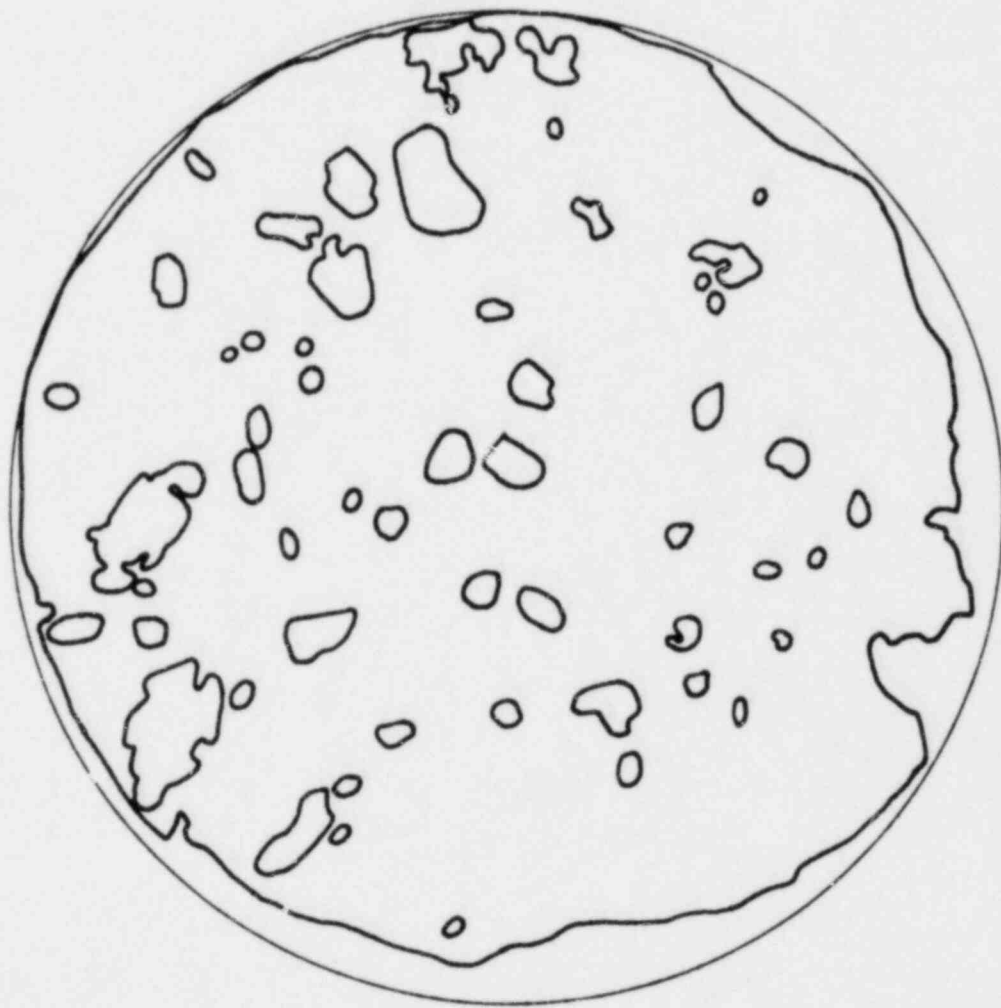


Figure 4a. Tracing of axial photograph of open tube. Gas velocity 16.7 m/s. Fluid quality 30%. For this photograph there was a medium wave height on the liquid film.

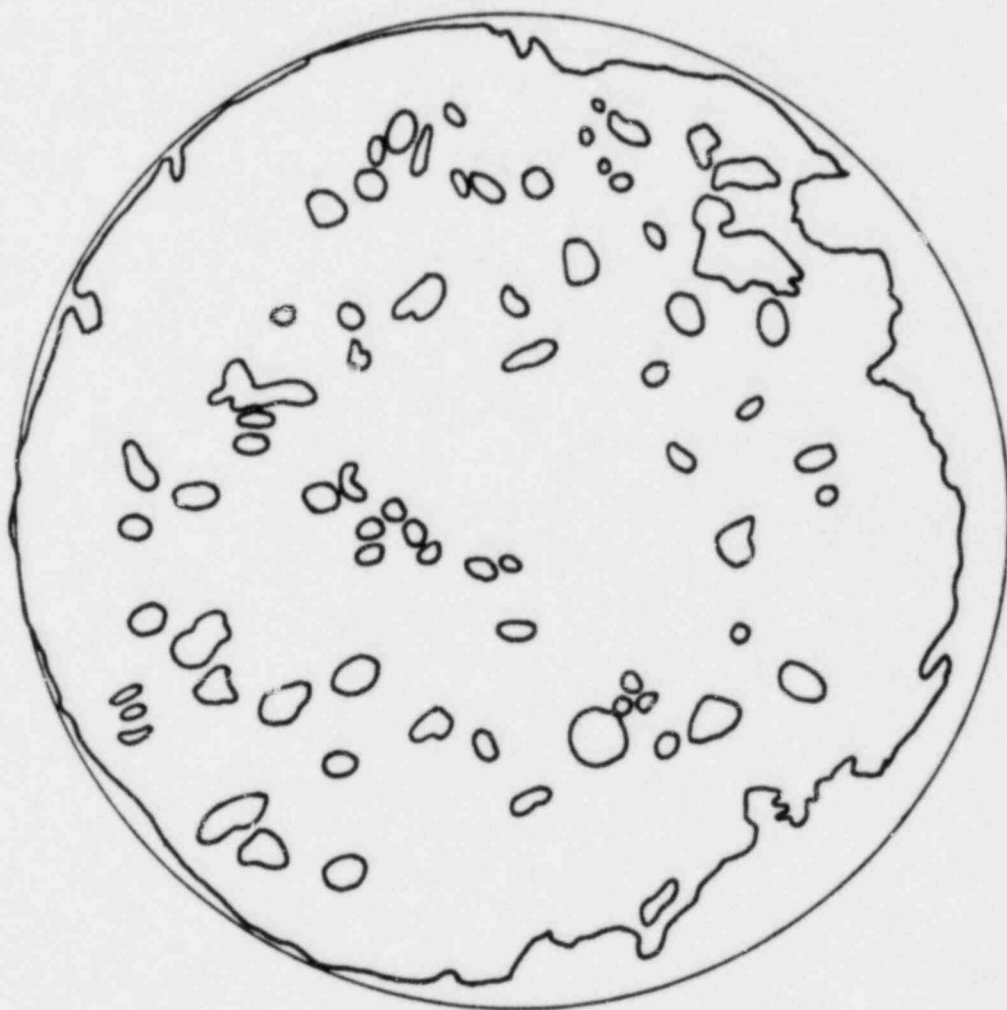


Figure 4b. Tracing of axial photograph of open tube. Gas velocity 16.7 m/s. Fluid quality 30%. For this photograph there was a medium wave height on the liquid film.

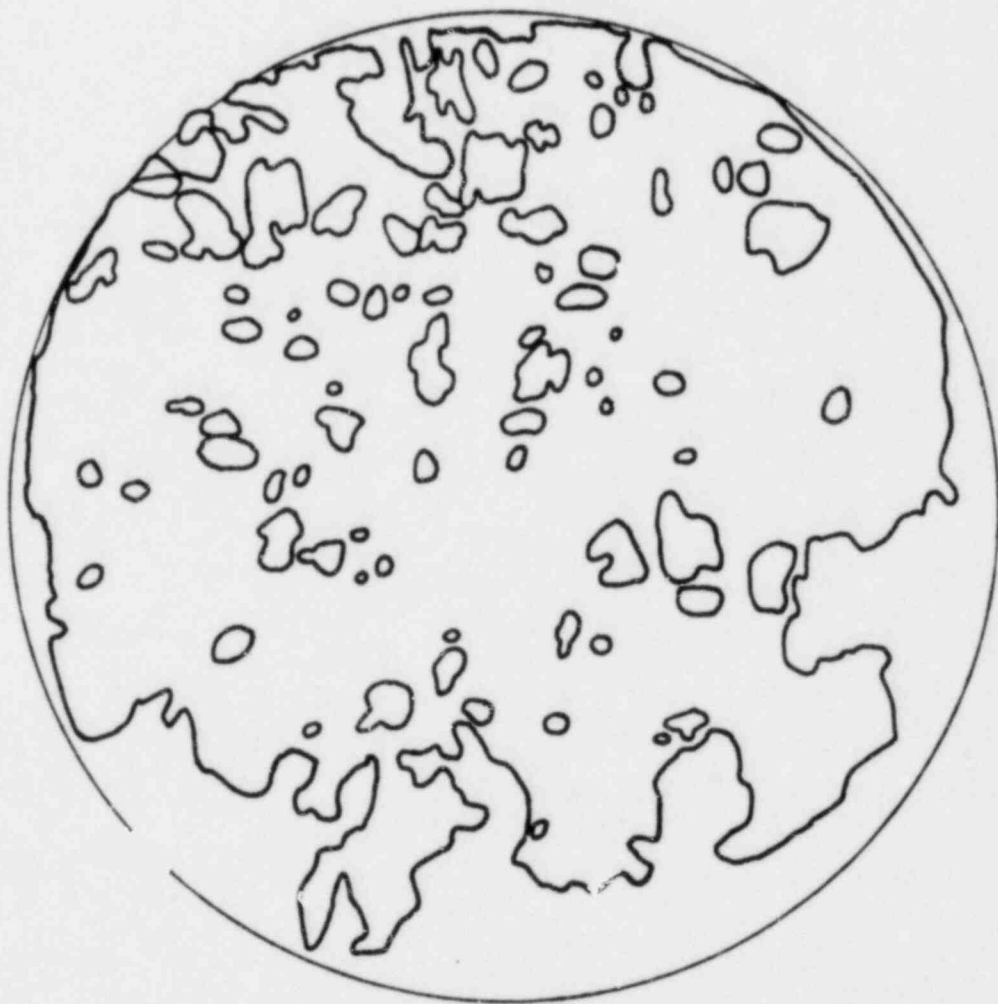


Figure 4c. Tracing of axial photograph of open tube. Gas velocity 16.7 m/s. Fluid quality 30%. For this photograph there was a medium wave height on the liquid film.

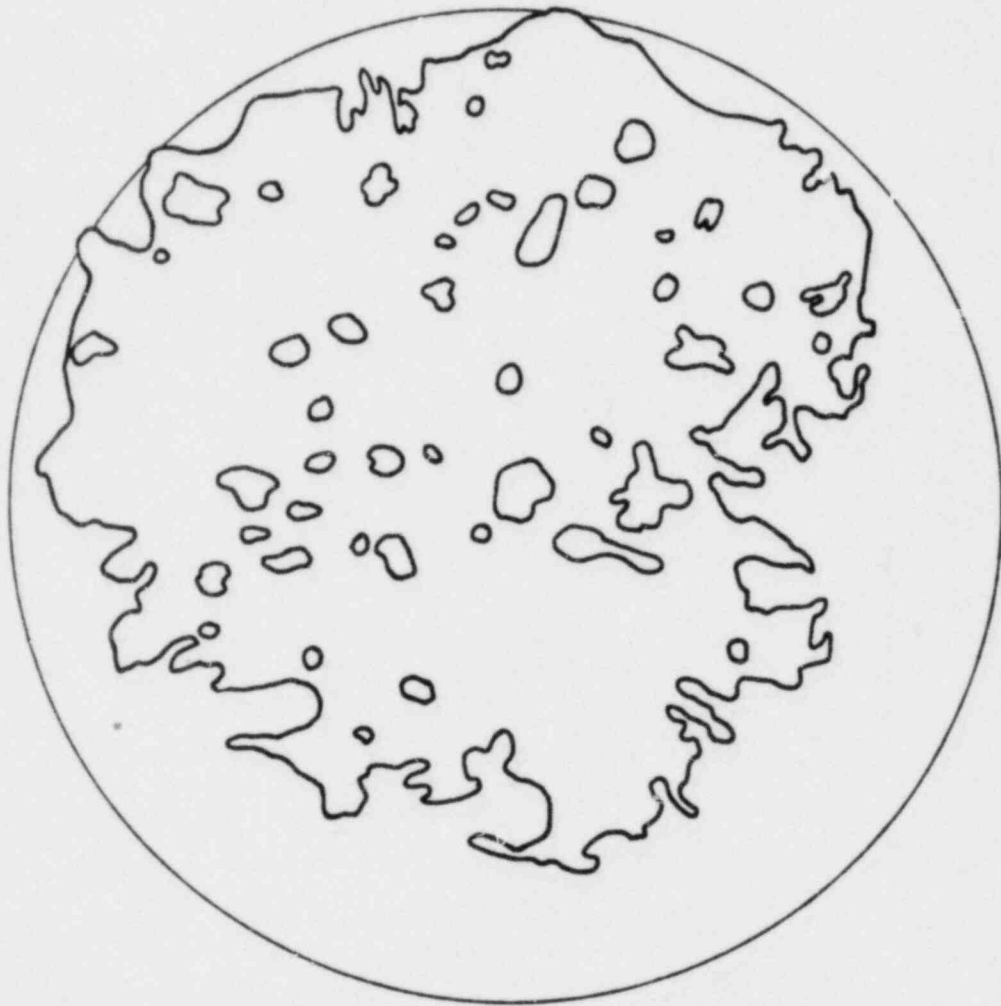


Figure 4d. Tracing of axial photograph of open tube. Gas velocity 16.7 m/s. Fluid quality 30%. For this photograph there was a maximum wave height on the liquid film.



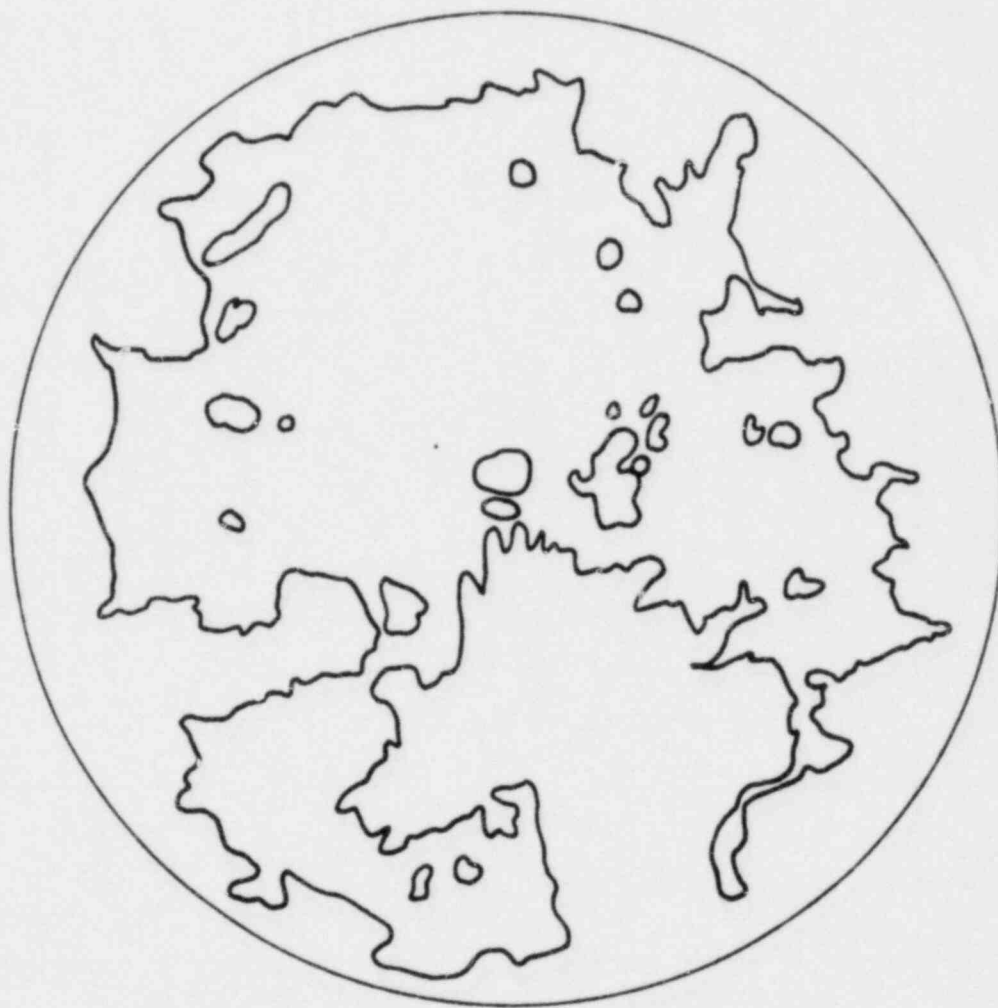


Figure 4e. Tracing of axial photograph of open tube. Gas velocity 16.7 m/s. Fluid quality 30%. For this photograph there was a maximum wave height on the liquid film.

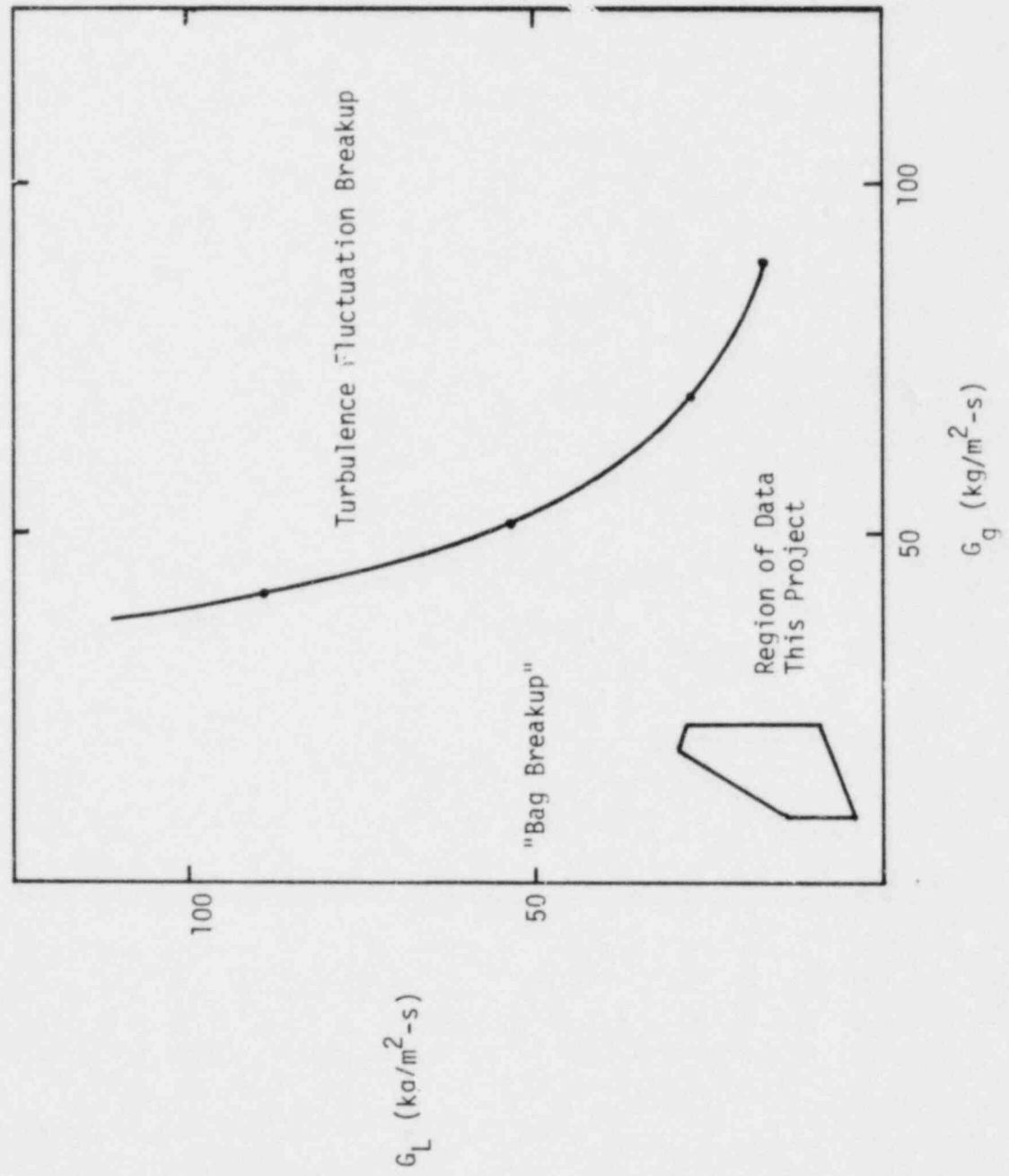


Figure 5. Division of droplet breakup mechanism from Azzopardi et al (1980).

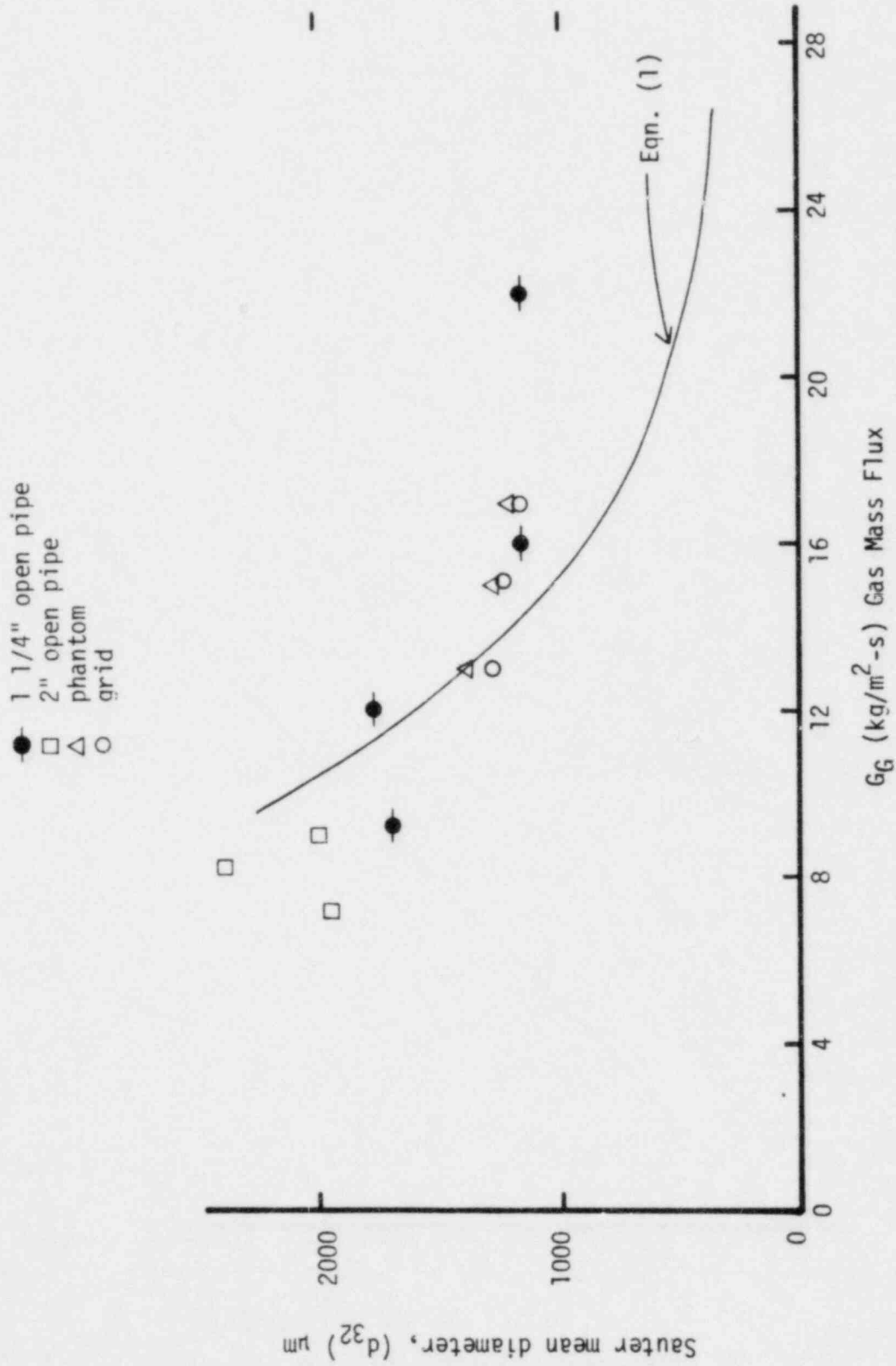


Figure 6. Comparison of experimental data with results from equation (1).

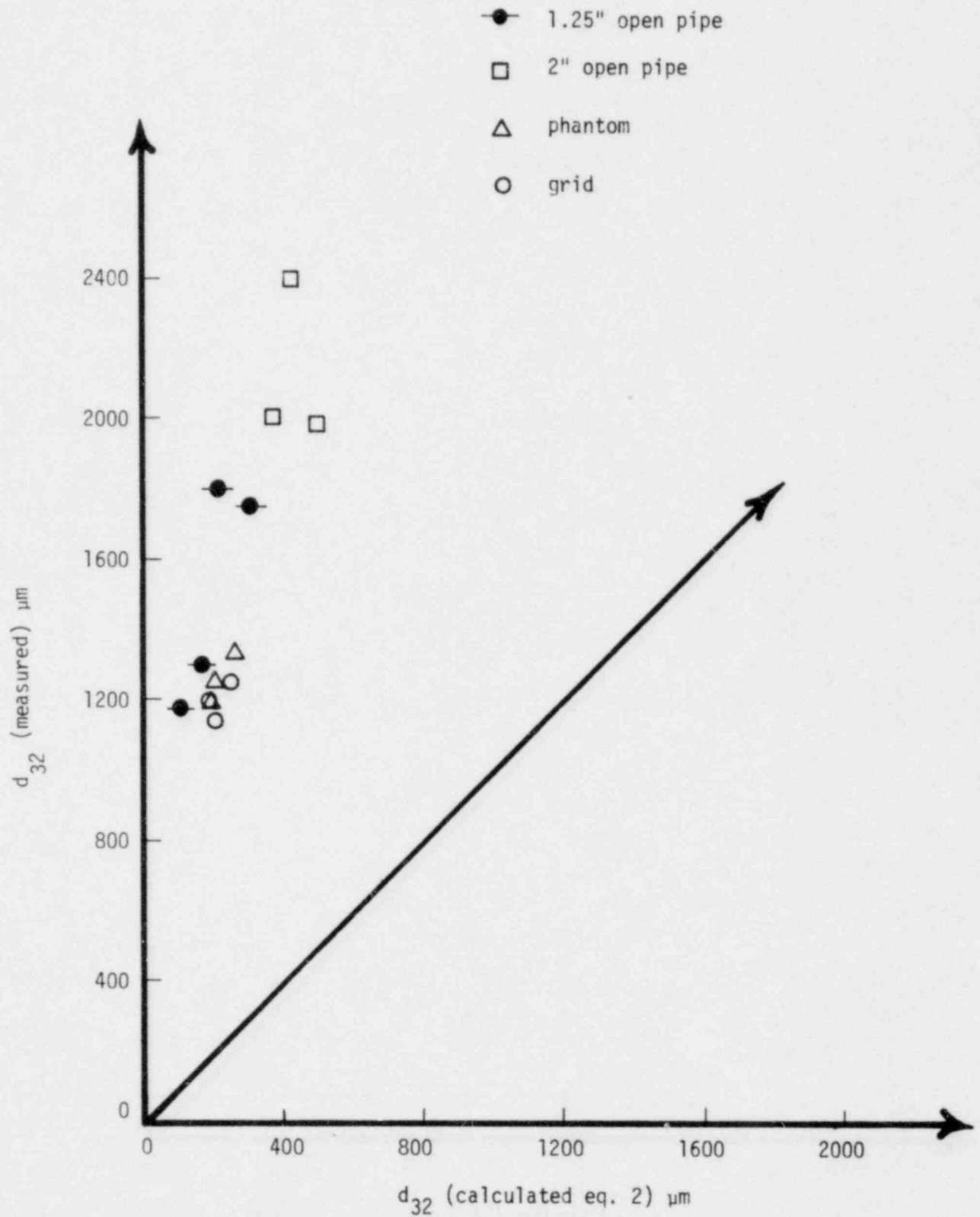


Figure 7. Comparison of experimental and calculated values of  $d_{32}$ . Turbulent fluxuation breakup as expressed by eq. (2) does not correlate data of this project. Calculations assume  $G_{LE} = 0.5 G_L$ .

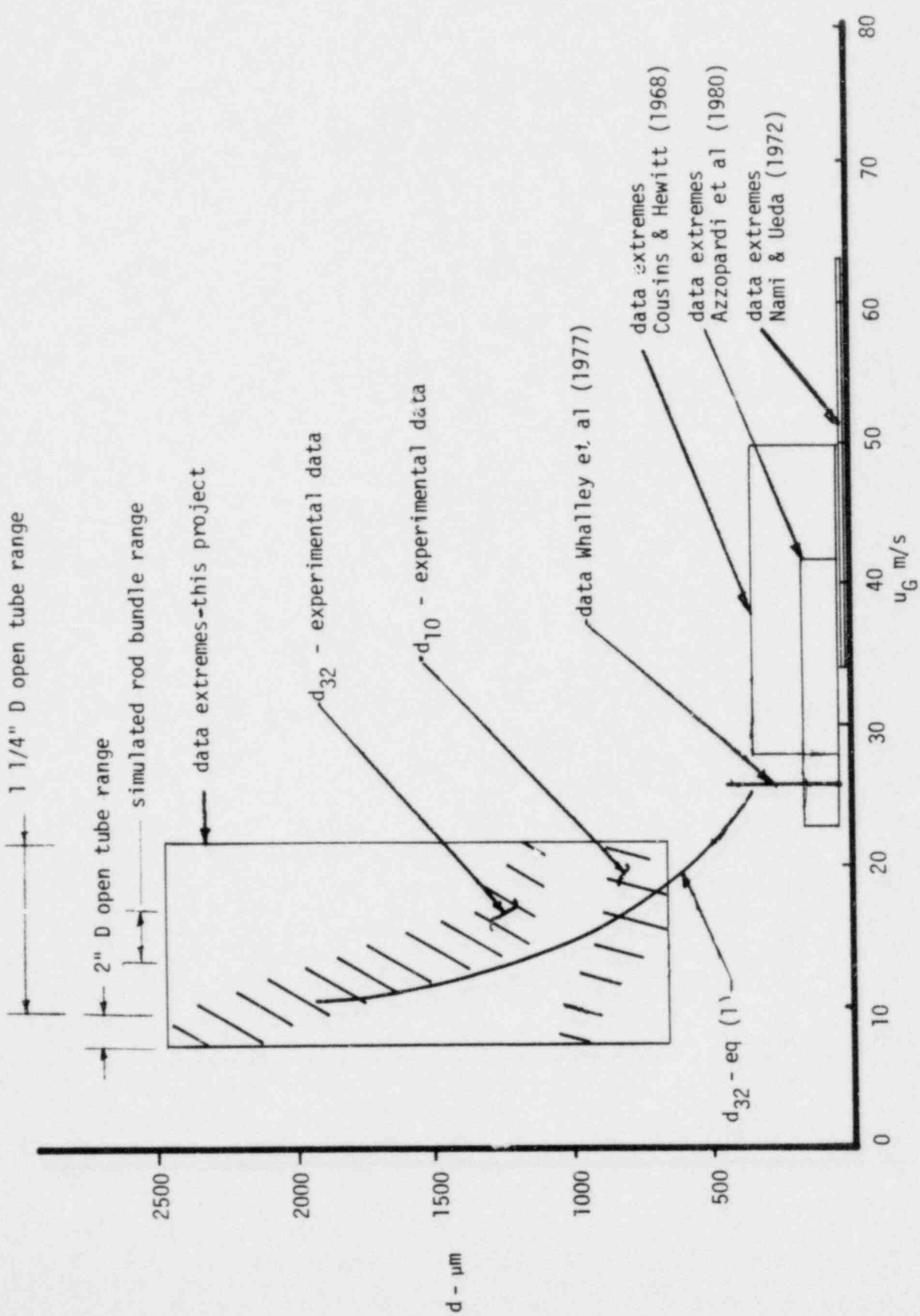


Figure 8. Comparison of all reported experimental data from similar systems (air-water) with predicted values from eq. (1) and with exponents of  $u_g$  of 1 and 2.



Figure 9. Droplet diameter ( $d_{10}$ ) ratios to show geometry effect (lower portion) and with hydraulic diameter ratio (upper portion).

GAS VELOCITY: 12.8 M/S

Rod Bundle Outlet — □

Rod Bundle Inlet - - - △

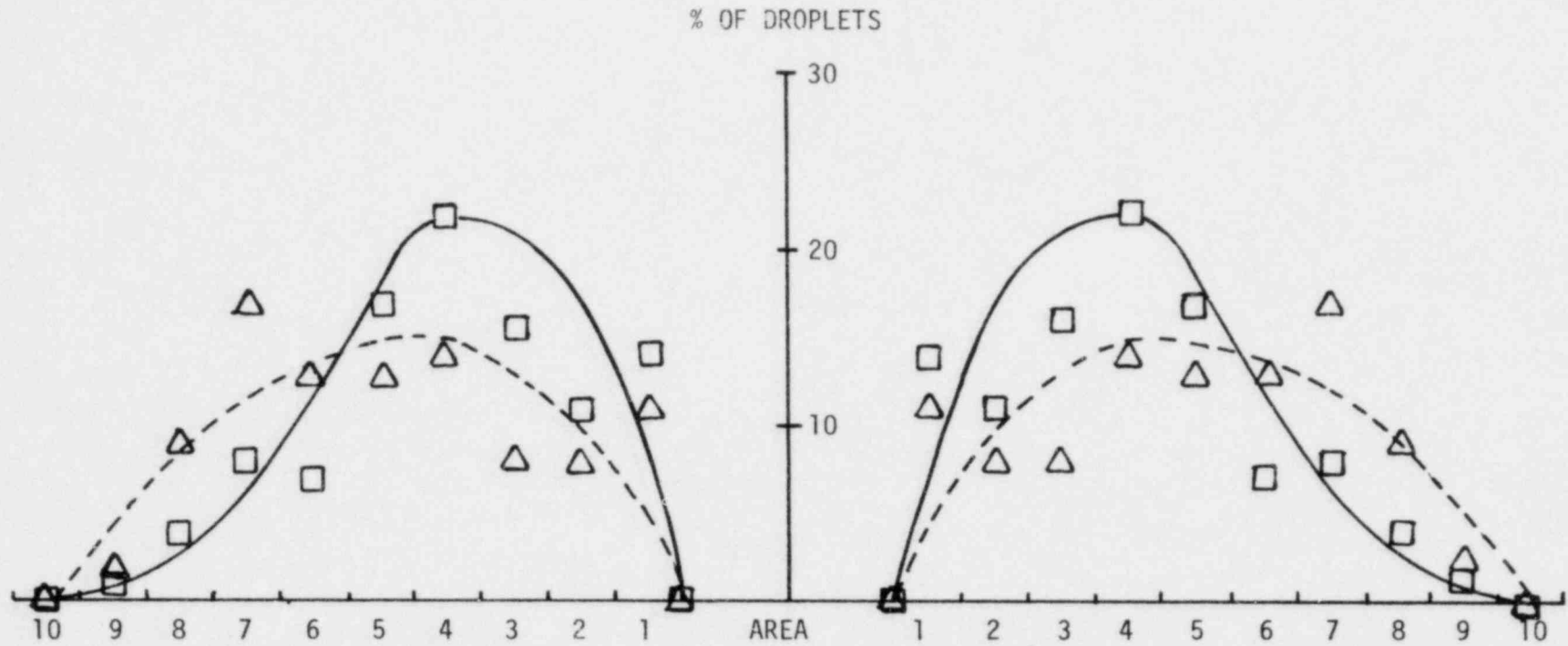


Figure 10. Droplet diameter distribution in flow cross section compared between rod bundle inlet and outlet. For area designation see Figure 13.

GAS VELOCITY: 14.5 M/S

Rod Bundle Outlet — □

Rod Bundle Inlet --- △

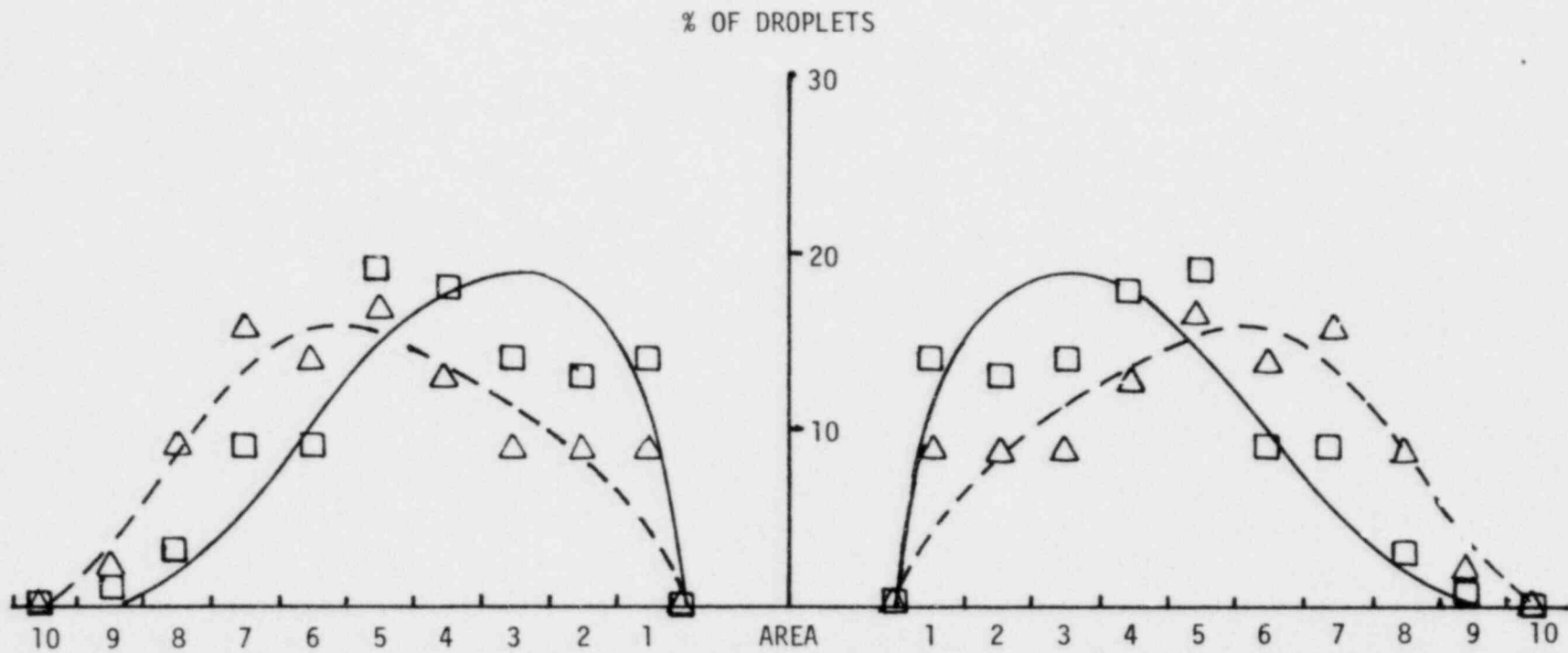


Figure 11. Droplet diameter distribution in flow cross section compared between rod bundle inlet and outlet. For area designation see Figure 13.



GAS VELOCITY: 16.1 M/S

Rod Bundle Outlet — □ —  
 Rod Bundle Inlet - - - △ - -

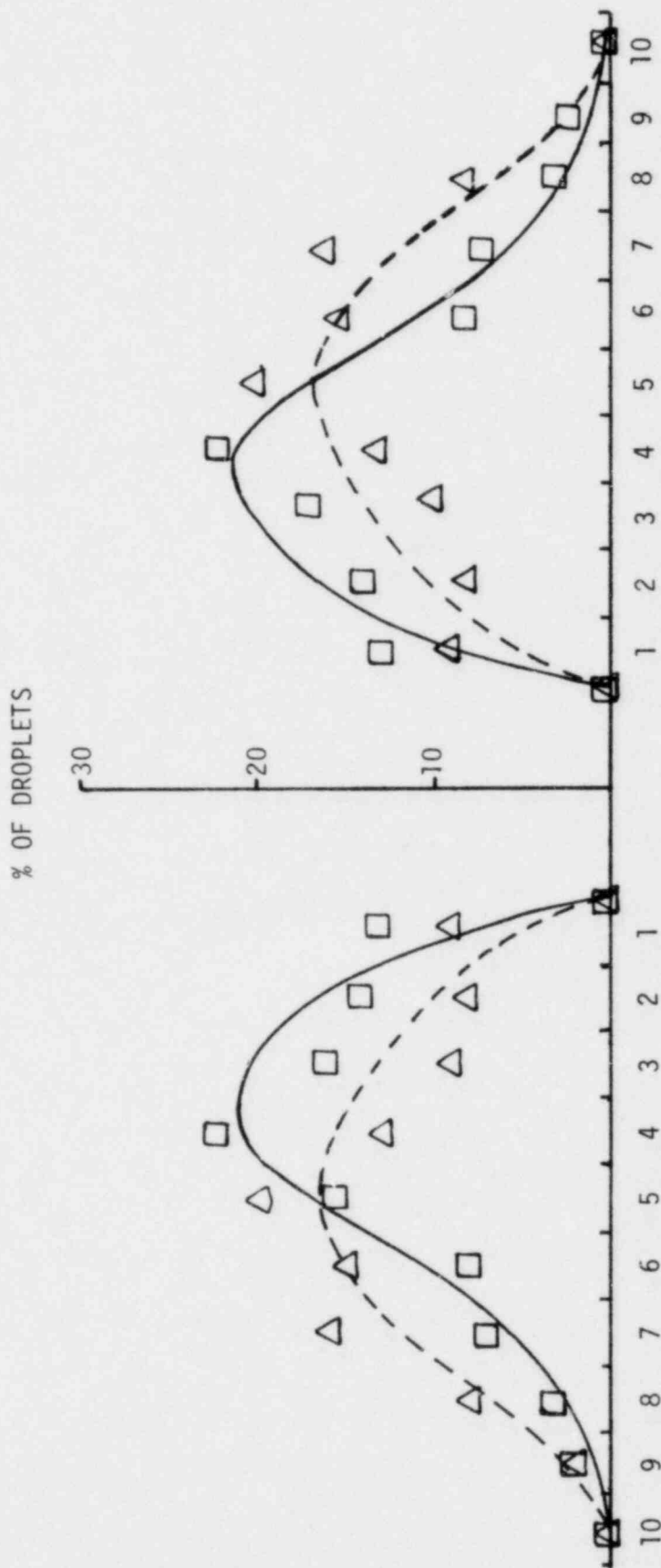


Figure 12. Droplet diameter distribution in flow cross section compared between rod bundle inlet and outlet. For area designation see Figure 13.

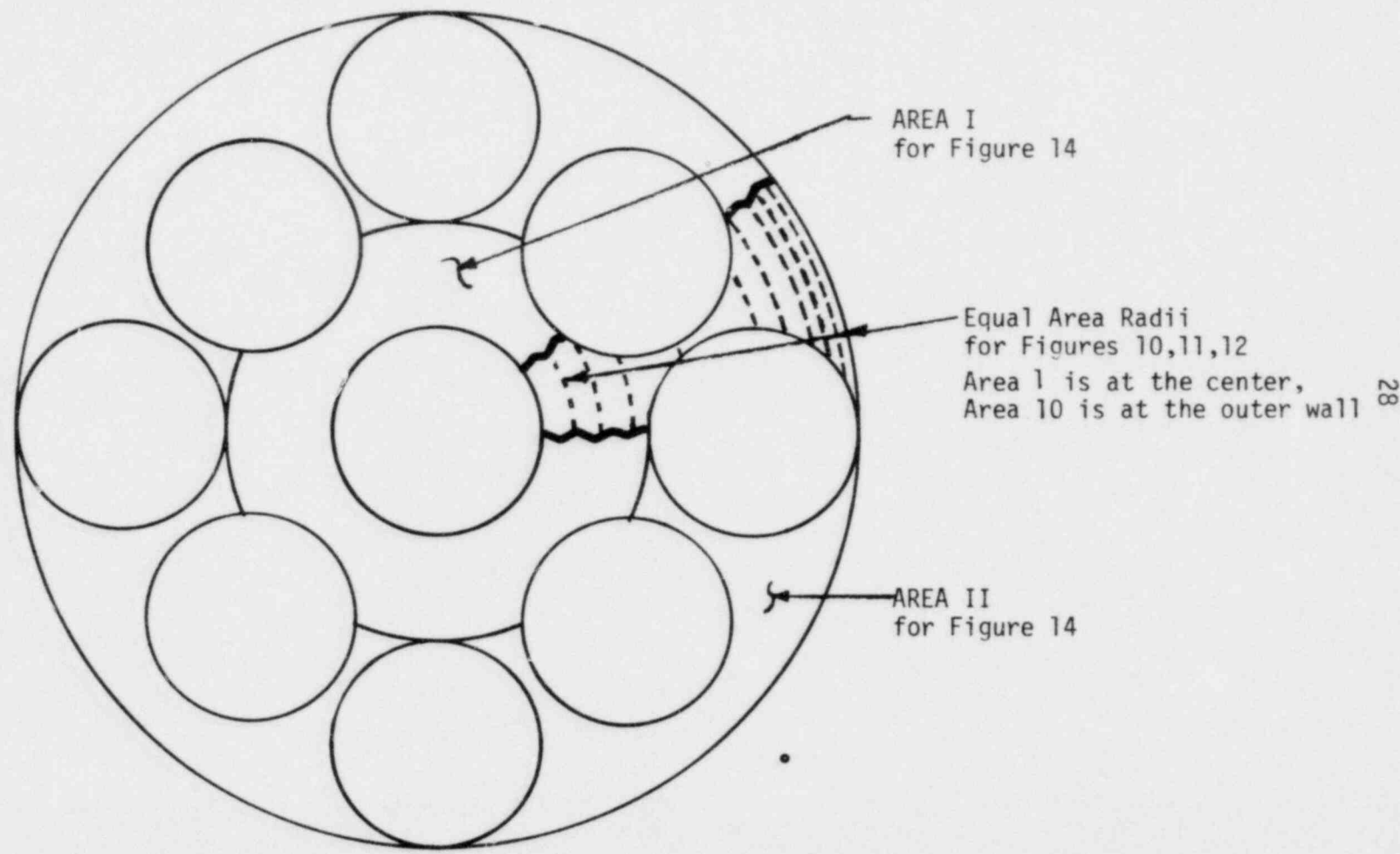


Figure 13. Flow area distributions for figures 10, 11, 12, and 14.

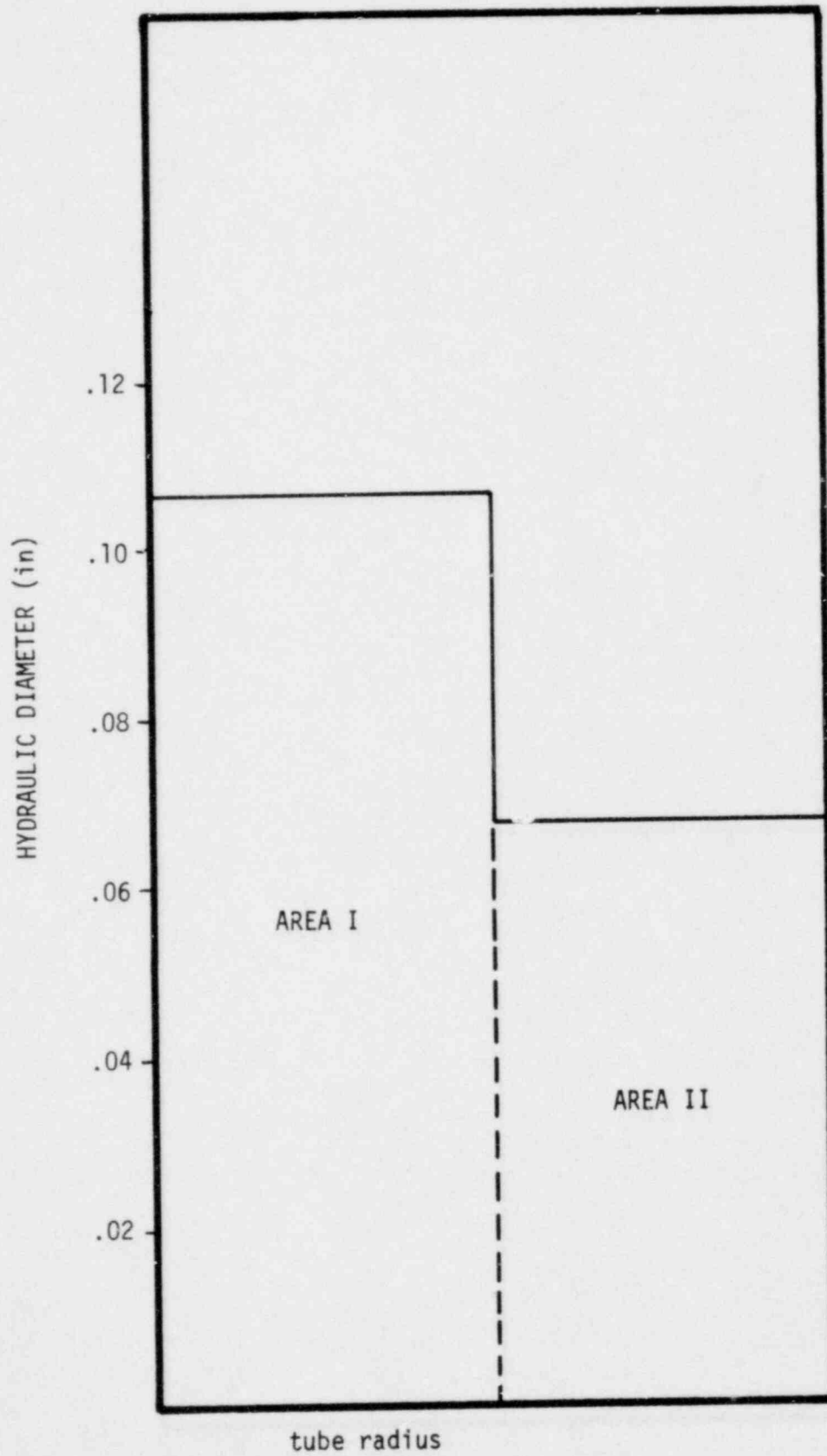


Figure 14. Hydraulic diameters for inner and outer areas of tube bundle. See Figure 13.

U.S. NUCLEAR REGULATORY COMMISSION  
BIBLIOGRAPHIC DATA SHEET

NU: EG/CR-2202

4. TITLE AND SUBTITLE (Add Volume No., if appropriate)  
Droplet Distributions in Open Pipes and Simulated Rod Bundles

2. (Leave blank)

3. RECIPIENT'S ACCESSION NO.

7. AUTHOR(S)  
R. V. Smith and R. D. Lindsted

5. DATE REPORT COMPLETED  
MONTH: November | YEAR: 1980

9. PERFORMING ORGANIZATION NAME AND MAILING ADDRESS (Include Zip Code)  
Department of Mechanical Engineering  
Wichita State University  
1845 Fairmount  
Wichita, KS 67208

DATE REPORT ISSUED  
MONTH: July | YEAR: 1981

6. (Leave blank)

3. (Leave blank)

12. SPONSORING ORGANIZATION NAME AND MAILING ADDRESS (Include Zip Code)  
Division of Accident Evaluation  
Office of Nuclear Regulatory Research  
U.S. Nuclear Regulatory Commission  
Washington, DC 20555

10. PROJECT/TASK/WORK UNIT NO.

11. CONTRACT NO.  
FIN B6250

13. TYPE OF REPORT  
Final

PERIOD COVERED (Inclusive dates)

15. SUPPLEMENTARY NOTES

14. (Leave blank)

16. ABSTRACT (200 words or less)

Results of droplet size distributions are reported for varying conditions of air-water flow and conduit geometry. Geometry variations were open pipe and the pipe containing simulated nuclear rod bundles with various support structures.

The experimental tests showed the gas velocity to be the primary variable influencing droplet size. The Hinze (1949) expression generally predicted the effective droplet size as a function of lower gas velocities. The Hinze (1949) correlation, however, showed the droplet size as a function of  $u_g^2$ . The exponent (2) appeared to be too high.

At higher gas velocities, the Hinze (1949) correlation failed and this appeared to indicate a change in the breakup mechanism for the higher gas velocities.

The droplet size change with respect to changes in geometry and mixture quality was small. It fell in the general range of the uncertainty for the data.

17. KEY WORDS AND DOCUMENT ANALYSIS

17a. DESCRIPTORS

17b. IDENTIFIERS/OPEN-ENDED TERMS

18. AVAILABILITY STATEMENT

Unlimited

19. SECURITY CLASS (This report)  
Unclassified

21. NO OF PAGES

20. SECURITY CLASS (This page)  
Unclassified

22. PRICE  
\$